Numerical Simulation of Conjugate Heat Transfer in Forced Convective Boundary Bilayered Cylindrical Pipe with Different Peclet Numbers

Oluwasegun S. Omosehin and *Adekunle O. Adelaja

[1] Department of Mechanical Engineering, University of Lagos, Akoka, Yaba, Lagos State, 101017, Nigeria
omosehin_oluwasegun@yahoo.com | aadelaja@unilag.edu.ng

Abstract - The heat transfer performance of bilayered composite systems through which thermally developing laminar fluids flow for cases in which axial conduction is either significant or negligible has been investigated. The heat transfer problems considered as two dimensional conjugate problems with appropriate boundary conditions were solved via computational fluid dynamics (CFD) approach in ANSYS 16.0. A parametric study was conducted to investigate the effects of Péclet number (*Pe*), ratio of the thermal conductivity of the laminate composite (k_{21}) and the laminate composite dimensionless-thickness ratio (η_{21}) on the wall-fluid interfacial temperature and interfacial heat flux for *Pe* of 5, 100 and 1000, η_{21}varying between 0.4 and 1.6, *Bi* of 5, k_{wf} of 20, k_{21} between 0.025 and 1, and η_1 of 0.71. The effect of *Pe* was found to be more pronounced on the interfacial heat flux. Also, the changes in k_{21} and η_{21}were shown to reduce with reduction in *Pe*.

Keywords - Composite cylinder, convective heat transfer, Numerical simulation; thick-walled pipes

1 INTRODUCTION

Bilayered cylindrical pipes are widely used for thermal insulation in oil- and gas-pipeline facilities to minimize the rate of heat loss and to prevent wax and hydrate formation during the conveyance of hot fluids between reservoirs and discharge units, especially in cold environments. Laminated material also has numerous applications in pressure vessels, aerospace components, naval structures, electronic equipment, and in the metal-forming and -rolling industries. They are very effective for design flexibility, increased strength-to-weight ratios, and dimensional stability under thermal loading, corrosion resistance, impact resistance, and high-fatigue strength.

Pe however is the ratio of the rate of advection of a physical quantity by the flow to the rate of diffusion of the same quantity. The parameter (*Pe*) is used to characterize fluid flow and flow conditions into three regimes. A low Peclet number ($Pe \leq 50$) describes a flow regime that accommodates both axial and radial conductions in the fluid, for instance, low Prandtl number flow in a single thick-walled cylinders (Darici et al. 2015; Ate et al., 2010). When $Pe = 100$, the length of the heating zone around the flow is considered short (Weigand and Lauffer, 2004), and for turbulent pipe flow (Lee, 1982). For very high $Pe = 1000$, axial conduction in the fluid is considered negligible Low *Pe* flows are often regarded as flows involving low Prandtl numbers and/or flows with low Reynolds numbers such as liquid metals.

Axial conduction cannot be neglected in these types of fluid flows. Also, in thick-walled pipes, wall axial conduction cannot be neglected. However, as wall thickness becomes extremely thin, wall axial conduction can be negligible. When *Pe* increases, wall and fluid axial conduction decrease and become negligible at high value. This can be approximated to the no axial-conduction condition case. Faghri and Sparrow (1980) in reported that interfacial heat flux is more informative in characterizing fluid flow than Nusselt number. Additionally, from literature, in relation to analysis of flow in single channels and over flat plates, few studies have been conducted on conjugate heat transfer in multilayered composite cylindrical pipes or slabs.

*Corresponding Author

For instance, some investigations have been done on the thermo-mechanical and mechanical properties of composite laminates (Chao et al. 2007; Pradeep and Ganesan, 2008). Therefore, the present work is centred on adaptation of wall-fluid interfacial temperature and heat flux distribution for the characterization of conjugate heat transfer dynamics in bilayered cylindrical pipe. Norouzi and AmiriDelouei (2015) and Lu et al. (2006) presented detailed reviews of the thermal analysis of multilayer composites. But, it is equally expedient that some explorations of few existing works on conduction heat transfer in multilayered composite as well as conjugate heat transfer in single and multilayered composite is undertaken. This is imperative in order to establish the landscape of research in conjugate heat transfer in multi-layered composite structure.

Yuen (1994) investigated the transient temperature distribution in a multilayered medium representing hot processing of flat plates subject to radiative surface cooling. Johansson and Lesnic (2009) employed the method of fundamental solutions to obtain the temperature field in transient heat conduction problems in layered materials. Tarn and Wang (2003, 2004) studied heat conduction in functionally graded and composite laminated cylinders. Torabi and Zhang (2015) investigated the temperature distribution and entropy generation rate within two-layer composite walls with combined convection and radiation boundary conditions. The thermal conduction and internal heat generation were assumed to be temperature dependent. The differential transformation method (DTM) was employed to solve the non-linear problem. It was shown that the ratio of the thermal conductivity and the interfacial location has a great effect on the rate of total entropy generation. De Monte (2003, 2004) investigated the heat conduction in homogeneous materials for one-dimensional and two-dimensional problems using the separation of variables method.

On two dimensional analysis of a single hollow cylinder, Zhang *et al*. (2010) numerically studied the effect of two-dimensional wall conduction in a thick-walled hollow cylinder with simultaneously developing laminar flow subjected to constant outside wall temperature. It was observed that for $k_{wf} \leq 25$, increasing δ/ri and decreasing

k_{wf} make the inner wall surface approach the uniform heat flux condition. In a related work, Adelaja *et al*. (2014) analyzed the effect of two-dimensional axial wall and fluid conduction for laminar flow in a thick-walled hollow cylinder subjected to convective boundary condition. Result showed that increasing η decreased the convective loss while increasing *Bi* and k_{wf} increased it.

Darici *et al*. (2015), and Altun *et al*. (2016) presented a finite difference numerical simulation of two-dimensional transient conjugate heat transfer in thermally developing laminar flow through a hollow thick-walled cylinder subjected to various boundary conditions. The boundary conditions considered in these works include insulation upstream and constant heat flux downstream, conductive boundary and periodically varying wall temperature respectively. Further, Alves *et al*. (2012) investigated conjugate heat transfer in multilayered composite pipes as a one-dimensional problem in the radii coordinate and the conveyed fluid equally as one-dimensional but in the axial coordinate. The heat transfer problem was solved numerically in a Fortran 90 environment while the structural problem was handled by commercially available CFD software ANSYS 11.0.

It is clear from the foregoing literature review that there are limited studies on the effect of fluid properties and laminate geometry on two-dimensional conjugate heat transfer of fluid flow through composite systems with convective boundaries. This, therefore, is the objective of the present study.

2 Problem Formulation

The schematic of the single regional bi-layered cylinder and the coordinate system considered is shown in Fig. 1. The composite medium consists of 2 - concentric cylindrical layers. Each layer is considered to be homogeneous, isotropic and with constant thermal properties. The physical problem investigates a fluid with temperature T_f in laminar flow with inlet velocity u_{in} flowing into a circular composite pipe comprising two layers in perfect thermal contact. The finitely long structure has an inner diameter d_i, the thickness of the first layer is (r_1 - r_i) and that of the second layer is (r_o – r_1). The structure is surrounded by ambient temperatureT_∞. The temperature of the fluid at entry is T_{in} and uniform. The temperature of the laminate at z = 0 and z = L are assumed to be adiabatic. Heat is transferred from the flowing fluid into the first layer and between the layers by conduction and from the second layer to the environment by convection.

The physical properties of the fluid and laminate are assumed to be constant. Further assumptions adopted are that: (1) the flow is steady and the fluid is incompressible; (2) the flow is laminar; (3) the radiative heat transfer, body and electrostatic forces, are negligible; (4) negligible heat generation due to viscous dissipation; and (5) there is no slip flow and no temperature jump.

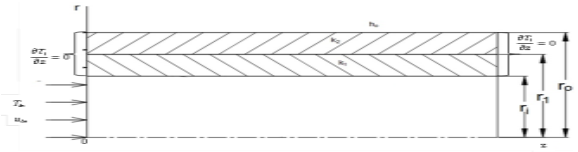

Fig. 1: Schematic diagram of laminated hollow cylinders.

Based on the aforestated assumptions, the mathematical representation of the physical model is based on continuum models of continuity, momentum, and energy. The dimensionless version of the governing partial differential equations that describe the steady state problem are presented in the continuity equation (Eq. (1)), the two-dimensional momentum equations (Eq. (2) and Eq. (3)) and the two-dimensional energy equations for the liquid and composite laminates (Eq. (4) - Eq. (6)), respectively with the appropriate boundary conditions provided in (Eq. 7 a - h)

Continuity equation

$$\frac{\partial U}{\partial Z}+\frac{1}{R}\frac{\partial (RV)}{\partial R}=0 \quad (1)$$

Momentum equation

$$\frac{\partial (UU)}{\partial Z}+\frac{1}{R}\frac{\partial (RUV)}{\partial R}=-\frac{\partial P}{\partial Z}+\frac{\partial}{\partial Z}\left(\frac{2}{Re}\frac{\partial U}{\partial Z}\right)+\frac{1}{R}\frac{\partial}{\partial R}\left(R\frac{2}{Re}\frac{\partial U}{\partial R}\right) \quad (2)$$

$$\frac{\partial (UV)}{\partial Z}+\frac{1}{R}\frac{\partial (RVV)}{\partial R}=-\frac{\partial P}{\partial R}+\frac{\partial}{\partial Z}\left(\frac{2}{Re}\frac{\partial V}{\partial Z}\right)+\frac{1}{R}\frac{\partial}{\partial R}\left(R\frac{2}{Re}\frac{\partial V}{\partial R}\right)-\frac{2}{Re}\frac{V}{R^2} \quad (3)$$

Energy equation

$$\frac{\partial (U\theta_f)}{\partial Z}+\frac{1}{R}\frac{\partial (RV\theta_f)}{\partial R}=\frac{\partial}{\partial Z}\left(\frac{2}{Pe}\frac{\partial \theta_f}{\partial Z}\right)+\frac{1}{R}\frac{\partial}{\partial R}\left(R\frac{2}{Pe}\frac{\partial \theta_f}{\partial R}\right) \quad (4)$$

Layer 1: $$\frac{\partial}{\partial Z}\left(k_{wf}\frac{2}{Pe}\frac{\partial \theta_1}{\partial Z}\right)+\frac{1}{R}\frac{\partial}{\partial R}\left(k_{wf}R\frac{2}{Pe}\frac{\partial \theta_1}{\partial R}\right)=0 \quad (5)$$

Layer 2: $$\frac{\partial}{\partial Z}\left(\frac{k_2}{k_{21}k_f}\frac{2}{Pe}\frac{\partial \theta_2}{\partial Z}\right)+\frac{1}{R}\frac{\partial}{\partial R}\left(\frac{k_2}{k_{21}k_f}R\frac{2}{Pe}\frac{\partial \theta_2}{\partial R}\right)=0 \quad (6)$$

where $k_w = k_1$ and

Dimensionless boundary conditions

$$Z=0;0\le R\le 1, U=1, V=0, \theta_f=1 \quad (7a)$$

$$Z=0;1\le R\le 1+\eta_1+\eta_2, U=0, V=0, \frac{\partial \theta_i}{\partial Z}=0 \quad (7b)$$

$$z=\frac{L}{r_i};0\le R\le 1, \frac{\partial U}{\partial Z}=0, v=0, \frac{\partial \theta_f}{\partial Z}=0 \quad (7c)$$

$$z=\frac{L}{r_i};1\le R\le 1+\eta_1+\eta_2, U=0, V=0, \frac{\partial \theta_i}{\partial Z}=0 \quad (7d)$$

$$R=0;0\le Z\le \frac{L}{r_i}, \frac{\partial U}{\partial Z}=0, V=0, \frac{\partial \theta_f}{\partial R}=0 \quad (7e)$$

$$R=1;0\le Z\le \frac{L}{r_i}, U=0, V=0, \theta_w=\theta_f, \frac{\partial \theta_f}{\partial R}=k_{wf}\frac{\partial \theta_1}{\partial R} \quad (7f)$$

$$R=1+\eta_1;\ 0\le Z\le \frac{L}{r_i}, U=0, V=0, \theta_2=\theta_1, \frac{\partial \theta_1}{\partial R}=k_{21}\frac{\partial \theta_2}{\partial R} \quad (7g)$$

$$R=1+\eta_1+\eta_2;0\le Z\le \frac{L}{r_i}, U=0, V=0, \frac{\partial \theta_2}{\partial R}+\frac{Bi\theta_2}{2a}=0 \quad (7h)$$

where $a=1+\eta_1+\eta_2$

The non-dimensional parameter (Eq. (8)) are defined as

$$Z=\frac{z}{r_i}, R=\frac{r}{r_i}, U=\frac{u}{u_{in}}, V=\frac{v}{u_{in}}, \theta=\frac{T-T_\infty}{T_{in}-T_\infty}, \eta_1=\frac{r_1-r_i}{r_i},$$
$$\eta_2=\frac{r_o-r_1}{r_i}, \eta_{21}=\frac{\eta_2}{\eta_1}, P=\frac{p}{\rho_f u_{in}^2}, k_{21}=\frac{k_2}{k_1}, k_{wf}=\frac{k_w}{k_f},$$
$$Pe=Re*Pr=\frac{2r_i u_{in}\rho_f c_{pf}}{k_f}, Re=\frac{2r_i u_{in}\rho_f}{\phi_f} \quad (8)$$

where T_1, T_2, T_{in}, T_∞ are the laminate layer 1, layer 2, fluid inlet and ambient temperatures respectively; r_i, $r_1$and r_o are the radii of the inner wall at the wall-fluid interface, layer 1-layer 2 interface and the outer surface of layer 2 respectively; u_{in} is the fluid inlet velocity; ρ_f, c_{pf}, and ϕ_f are the fluid density, specific heat capacity, and dynamic viscosity respectively; k_f, k_1 (=k_w) and k_2 are the thermal conductivities of the fluid, layer 1 (also referred to as wall) and layer 2 respectively. The dimensionless parameters are noted, thus θ is dimensionless temperature, *Pe* is the Péclet number, *Bi* is the Biot number, k_{wf} the ratio of the thermal conductivity of layer 1-to-fluid, while k_{21} is the ratio of the thermal conductivity of layer 2 to layer 1, η_1 and η_2 are the thickness ratios of laminate layer 1 and layer 2 respectively, $\eta_{21}$is the thickness ratio of layer 2 to layer 1, *Re, Pr* and *P* are the Reynolds number, Prandtl number, and dimensionless pressure respectively.

The dimensionless fluid bulk temperature θ_b, dimensionless wall-fluid interfacial heat flux and q'_{wi} Nusselt number *Nu* (Zhai et al., 2017) can be calculated in (Eq. 9a - c).

$$\theta_b = 4\int_0^1 R(1-R^2)\theta_f dR \quad (9a)$$

$$q'_{wi} = -\left(\frac{\partial\theta_f}{\partial R}\right)_{R=1} \quad (9b)$$

$$Nu = \frac{d_i\frac{\partial T_f}{\partial R}\Big|_{R=r_i}}{T_b - T_{wi}} \quad (9c)$$

The theoretical hydrodynamic and thermal entrance lengths are respectively presented in Eq. 10a, b (Burmerister, 1983).

$$L_H = 0.1Re_D r_i;\ L_T = 0.1Re_D Pr * r_i \quad (10a, b)$$

3 Numerical Method and Validation

In this study, commercially available CFD software, ANSYS Fluent 16.0, was used to solve the governing partial differential equations with the imposed boundary conditions. Additionally, a temperature inlet and a velocity inlet were prescribed as the fluid-inlet boundary conditions, and a pressure- outlet was prescribed as the outlet boundary condition. The governing partial differential equations and the imposed boundary conditions were discretized using the finite volume method (FVM). The semi-implicit method for pressure-linked equations (SIMPLE) scheme algorithm was employed for the pressure-velocity coupling. During the numerical simulation, the fluid and the laminated media were treated as one body – computational domain - with different thermo-physical properties.

The interface condition between the fluid and laminate layer 1 was not specified because the computation was of conjugated types. Fig. 2 shows the computational mesh for the fluid and composite system used for the study. The grids in the radial direction are not uniform, while they are uniform in the axial direction. The fluid is meshed with tetrahedral cells in the radial and cut cells in the axial with refinement at the wall-fluid interface, while the laminate is meshed with cut cells both radially and axially. It has been reported that for conjugate problems with convective boundary, the Nusselt number lies between the experimental and analytical constant temperature value (3.66) and the constant heat flux value (4.364) (Darici et al, 2015). The current study confirmed this, as shown in Fig. 3a. The grid-independent study was conducted for a suitable grid density using the same figure while iterations continued until convergence of root mean square residual for all variables were less than 10^{-6}. The result showed that the number of elements (845162) used is adequate and the errors, reported in Table 1, range between 0.18% and 0.52% when increased from 439163 to 845162 and from 845162 to 1661728 respectively. The Nusselt number was obtained by using water in laminar flow as the working fluid while steel was used for the bilayered laminate. For further validation of the method of solution, numerical simulation was conducted for the case of water with constant properties in the laminar flow without the solid region but with constant heat flux over the entire wall surface. Under this condition, the reference analytical result of 4.364 (Kay and Crawford, 1993) was obtained as shown in Fig. 3b.

4 Results and Discussion

The results of the conjugate heat transfer analysis are presented in terms of the influence of certain parameters such as P*e*, k_{21}, and η_{21}on the bulk, wall-fluid interfacial temperatures as well as the wall-fluid interfacial heat flux. The axial distribution of the wall-fluid interfacial temperature and wall-fluid interfacial heat flux are presented for dimensionless thickness of layer 1 η_1 of 0.71, η_{21} ranging between 0.4 and 1.6; *Bi* of 5; k_{wf} of 20; *Pe* of 5, 100 and 1000; and k_{21} between 0.025 and 1 as captured in Table 2. The effect of *Pe* is clearly shown in Figs. 4 – 6 for $\eta_1$of 0.71as its decrease resulted in the unification of the heat flux as well as in the reduction in the wall-fluid interfacial and fluid bulk temperatures and heat flux downstream of the flow.

Fig. 4 highlights the contour of the fluid-wall interfacial temperature and heat flux for *Pe* of 5, 100 and 1000. The contour is aimed at creating visual effects of the intensity and the direction of heat flow as it varies with Péclet number. Figs. 4 a - c show that temperature gradient along the flow length reduces with increasing *Pe* so that the temperature downstream is higher for higher *Pe*. For the heat flux result, Figs. 4d – f, better heat flux is observed as *Pe* decreases. For *Pe* = 5 (Fig. 4d), there is a sudden increase in heat flux close to the entrance region because of the predominance of thermal diffusion. Further downstream, the heat flux continues to increases but at a lower rate. For *Pe* = 100 (Fig. 4e), temperature gradient inside the laminate structure steadily changes, thus a steady increase in the heat flux was obtained.

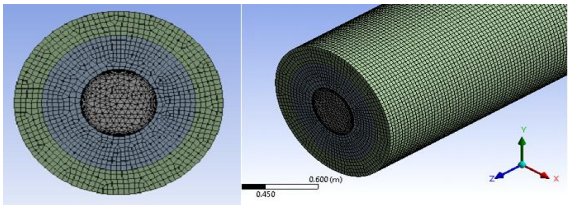

Fig. 2: Computational mesh of the fluid-laminate composite body.

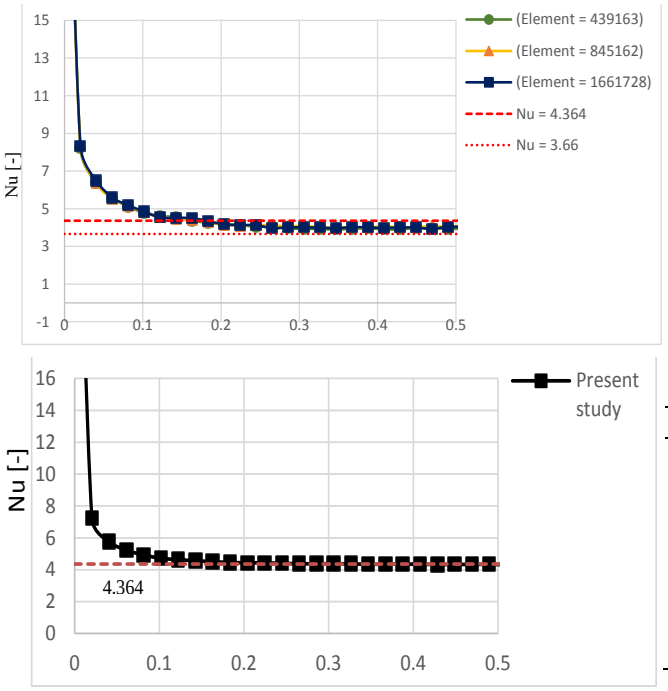

Fig 3 a) Grid independence study and result of Nusselt number, b) Validation with analytical heat flux value.

Table 1: Grid refinement result

Element Size	Nodes	$\frac{\left\|(Nu_j)_{ave} - (Nu_{j+1})_{ave}\right\| \times 100}{\left\|(Nu_j)_{ave}\right\|}$
439163	324512	-
845162	641268	0.518
1661728	1369445	0.178

j = number of attempts at grid refinement

Table 2: Dimensionless parameter used for simulation

	Parameter description	Parameter	Values
1	Layer 1 thickness	η_1	0.71
2	Layer 1-to-layer 2 thickness ratio	η_{21}	0.4 – 1.6
3	Biot number	Bi	3 – 30
4	Péclet number	Pe	5 – 1000
5	Layer 1 wall-to-fluid thermal conductivity ratio	k_{wf}	5 – 50
6	Layer 2-to-layer 1 thermal conductivity ratio	k_{21}	0.025 – 1.0

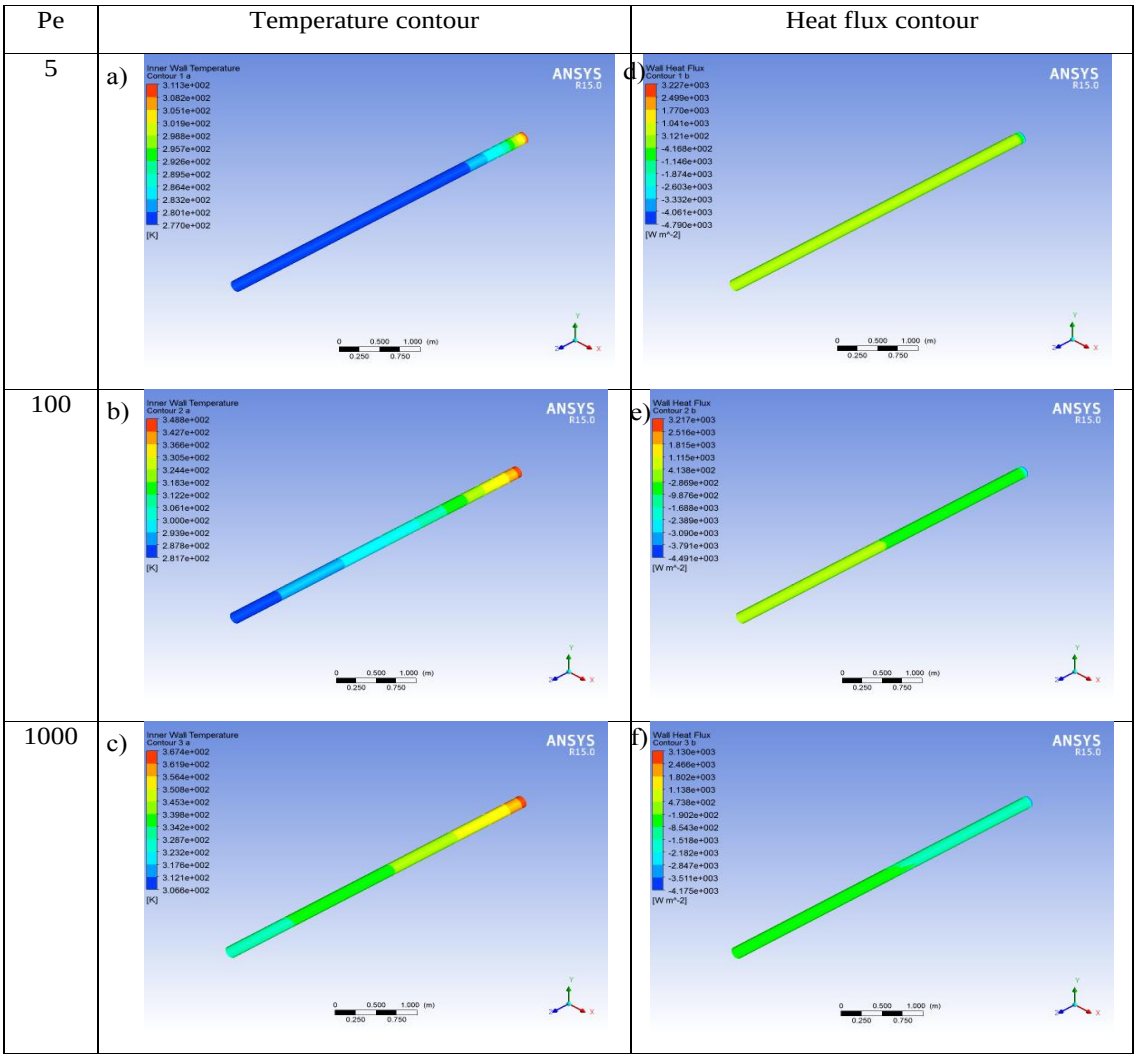

Fig. 4: The contours of the profiles of the wall-fluid interfacial temperature and heat flux for a) Pe = 5, b) Pe = 100 and, c) Pe = 1000.

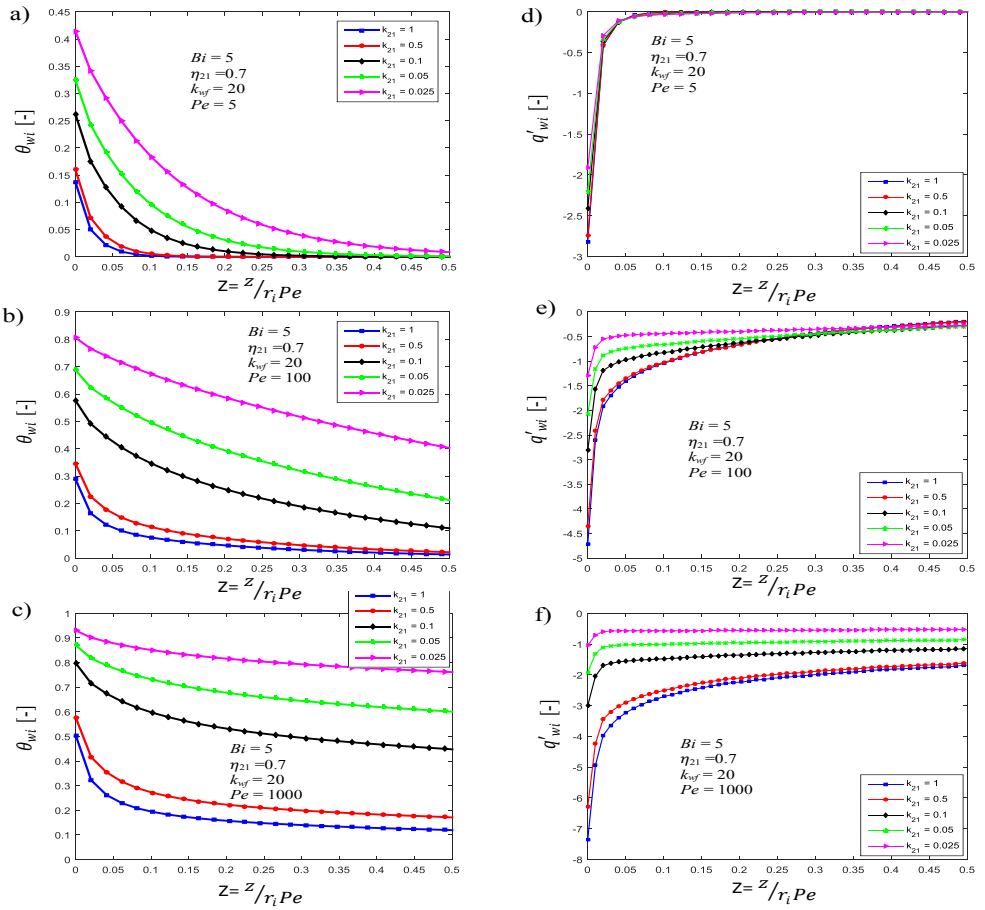

Fig. 5: The effect of the layer 2-to-layer 1 thermal conductivity ratio (k21) on the wall-fluid interfacial temperature (a – c) and interfacial heat flux (d – f) for kwf = 20, Bi = 5, η_{21} = 0.7 for (a & d) Pe = 5, (b & e) Pe = 100 and (c & f) Pe = 1000.

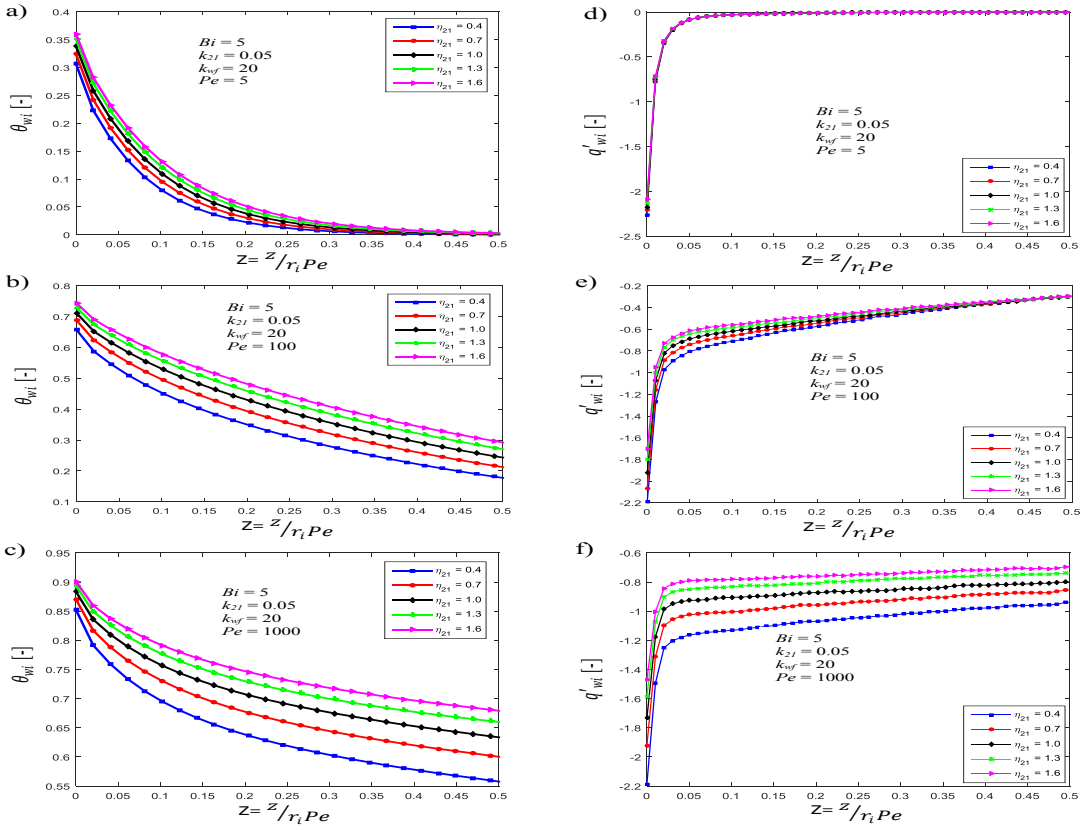

Fig. 6: The variation of wall-fluid interfacial temperature (a – c) and interfacial heat flux (d – f) along hollow cylindrical composite structure length for different thicknesses ratio for k21 = 0.05, Bi = 5, and kwf = 20 and for (a & d) Pe = 5, (b & e) Pe = 100 and (c & f) Pe = 1000.

There seems to be a significant increase in heat flux midway the flow to the exit. This may be attributed to the swing in dominance between the thermal and the momentum diffusivity. For Pe = 1000 (Fig. 4f), the temperature gradient is small hence the increase in heat flux is not as pronounced as it is for lower Pe. Fig. 5 reveals the results of the variation in the wall-fluid interfacial temperature (5a-c) and interfacial heat flux (5d-f) along the length of the pipe for different layer 2-to-layer 1 thermal conductivity ratios k_{21}, for Pe = 5 (a, d), Pe = 100 (b, e), and Pe = 1000 (c, f). The following parameters are kept constant: k_{wf} = 20, Bi = 5, η_{21} = 0.7 and η_1 = 0.71.

Increase in k_{21}corresponds to reduction in the thermal resistance of the laminate, such that for k_{21} = 1 the two materials are similar and behave as a single material. For reduced k_{21}, layer 2 serves as an insulator but becomes a conductor with increase. Generally, an increase in k_{21} reduces the interfacial temperature but increases the interfacial heat flux. Fig. 6 shows the variation in the wall-fluid interfacial temperature (6a-c) and wall-fluid interfacial heat flux (6d-f) for different dimensionless layer 2-to-layer 1 thickness ratios for Pe = 5 (a, d), Pe = 100 (b, e), and Pe = 1000 (c, f) while the following parameters were kept constant; k_{21} = 0.05, k_{wf} = 20, Bi = 5, and η_1 = 0.71. Increased η_{21} corresponds to increased thermal resistance. Therefore increased η_{21}reduced the heat flux across the laminate but increases the wall-fluid interfacial temperature. As Pe increases from 5 to 100, the region in which the effect of thickness ratio is insignificant moves from the upstream to downstream.

5 CONCLUSION

This study investigated numerically the thermal performance of thick-walled bilayered composite pipe through which thermally developing fluid flows with convective boundary conditions at the outer interface for the case in which Biot number of 5; wall-to-fluid thermal conductivity ratio of 20; layer 2-to-layer 1thermal conductivity ratio between 0.025 and 1; layer 2-to-layer 1 thickness ratio between 0.4 and 1.6; layer 1 thickness of 0.71 and Peclet number of 5, 100 and 1000. The effect of layer 2-to-layer 1 thermal conductivity ratio, layer 2-to-layer 1 thickness ratio and Peclet number were investigated on the wall-fluid interfacial temperature and heat flux and were found to be significant. For high Peclet number, Pe = 1000, the effect of axial conduction is negligible and an increase in layer 2-to-layer 1 thickness ratio results in an increase in the interfacial temperature and a decrease in the interfacial heat flux. An increase in layer2-to-layer1 thermal conductivity causes a decrease in interfacial temperature and an increase in the interfacial heat flux. The effect of Peclet number is seen to be more pronounced on the heat flux than on the temperature. Also, the effect of or change in k_{21} and η_{21} are seen to reduce with reduction in Pe. This is because axial conduction increases with decrease in Pe.

REFERENCES

Adelaja, A.O., Dirker, J., Meyer, J. P. (2014). Effects of the thick walled pipes with convective boundaries on laminar flow heat transfer. Appl. Energy 130, 838–845.

Altun, A. H., Bilir, S., Ates, A. (2016). Transient conjugated heat transfer in thermally developing laminar flow in thick walled pipes and minipipes with time periodically varying wall temperature boundary condition. Int. J. Heat Mass Transfer 92, 643–657.

Alves, L., Sousa, J. R. M., Ellwanger, G.B. (2012). Transient Thermal Effects and Walking in Submarine Pipeline. Int. J. Modeling Simulation Petroleum Industry 6 (1), 37 – 44.

Ates, A., Darıcı, S., Bilir, S. (2010). Unsteady conjugated heat transfer in thick walled pipes involving two-dimensional wall and axial fluid conduction with uniform heat flux boundary condition. Int. J. Heat Mass Transfer 53, 5058–5064.

Burmerister, L. C. (1983). Convective Heat Transfer, John Weily and Sons.

Chao, C.K., Che, F.M., Shen, M.H. (2007). An exact solution for thermal stresses in a three-phase composite cylinder under uniform heat flow. Int. J. Solids Struct 44, 926-940.

Darıcı, S., Bilir, S., Ates, A. (2015). Transient conjugated heat transfer for simultaneously developing laminar flow in thick walled pipes and minipipes. Int. J. Heat Mass Transfer 84, 1040–1048.

De Monte, F. (2004). Transverse eigen problem of steady-state heat conduction for multi-dimensional two-layered slabs with automatic computation of eigenvalues. Int. J. Heat Mass Transfer 47, 191–201.

De Monte, F. (2003). Unsteady heat conduction in two-dimensional two slab-shaped regions: Exact closed-form solution and results. Int. J. Heat Mass Transfer 46 (8), 1455–1469.

Faghri, M., Sparrow, E.M. (1980). Simultaneous wall and fluid axial conduction in laminar pipe-flow heat transfer. J. Heat Transfer 102, 58–63.

Johansson, B.T., Lesnic, D. (2009). A method of fundamental solutions for transient heat conduction in layered materials. Eng. Anal. Boundary Elements 33, 1362-1367.

Kays, W. M. Crawford, M. E. (1993). Convective heat and mass transfer. Third ed., McGraw-Hill, New York.

Lee, S. L. (1982). Forced convection heat transfer in low Prandtl number turbulent flows: influence of axial conduction. Can. J. Chem. Eng. 60, 482 – 486.

Lu, X., Tervola, P., Viljanen,M. (2006). Transient analytical solution to heat conduction in composite circular cylinder, Int. J. Heat Mass Transfer 49 (1–2), 341–348.

Norouzi, M., AmiriDelouei, A. (2015). Exact analytical solution for unsteady heat conduction in fiber-reinforced spherical composites under the general boundary conditions. J. Heat Transf. 137, 101701-1.

Pradeep, V., Ganesan, N. (2008). Thermal buckling and vibration behavior of multilayer rectangular viscoelastic sandwich plates. J. Sound Vibrat. 310, 169-183.

Tarn, J.Q., Wang, Y.M. (2003). Heat conduction in a cylindrically anisotropic tube of a functionally graded material. Chin J. Mech. 19, 365-372.

Tarn, J.Q., Wang,Y.M. (2004). End effects of heat conduction in circular cylinders of functionally graded materials and laminated composites. Int. J. Heat Mass Transfer 47, 5741-5747.

Torabi, M., Zhang, K. (2015). Heat transfer and thermodynamic performance of convective–radiative cooling double layer walls with temperature-dependent thermal conductivity and internal heat generation. Energy Convers Manag 89, 12–23.

Weigand, B., Lauffer, D. (2004). The extended Graetz problem with piecewise constant wall temperature for pipe and channel flows. Int. J. Heat Mass Transfer 47, 5303 – 5312.

Yuen, W. Y. D. (1994). Transient temperature distribution in a multilayer medium subject to radiative cooling, Appl. Math. Modelling 18, 93 – 100.

Zhai,L., Xu,G., Quan,Y., Song,G., Dong,B., Wu, H. (2017). Numerical analysis of the axial heat conduction with variable fluid properties in a forced laminar flow tube. Int. J. Heat Mass Transfer 114, 238-251.

Zhang, S-X., He, Y-L., Lauriat, G., Tao, W-Q. (2010). Numerical studies of simultaneously developing laminar flow and heat transfer in microtubes with thick wall and constant outside wall temperature. Int. J. Heat Mass Transfer 53, 3977–3989